

## Report

# Voltage-dependent anion channels (VDAC) in the plasma membrane play a critical role in apoptosis in differentiated hippocampal neurons but not in neural stem cells

Nesar Akanda,<sup>1,2,†</sup> Roshan Tofighi,<sup>2,†</sup> Johan Brask,<sup>1</sup> Christoffer Tamm,<sup>2</sup> Fredrik Elinder<sup>1</sup> and Sandra Ceccatelli<sup>2,\*</sup>

<sup>1</sup>Department of Clinical and Experimental Medicine; Division of Cell Biology; Linköping University; Linköping, Sweden; <sup>2</sup>Department of Neuroscience; Karolinska Institutet; Stockholm, Sweden

<sup>†</sup>These authors contributed equally to this work.

**Key words:** patch clamp, single-channel recordings, apoptosis, VDAC, hippocampal neurons, neural stem cells, sodium channels

One of the earliest morphological changes occurring in apoptosis is cell shrinkage associated with an increased efflux of K<sup>+</sup> and Cl<sup>-</sup> ions. Block of K<sup>+</sup> or Cl<sup>-</sup> channels prevents cell shrinkage and death. Recently, we found evidences for the activation of a voltage-dependent anion channel in the plasma membrane (pl-VDAC) of a hippocampal cell line undergoing apoptosis. Nothing is known on pl-VDAC in apoptotic cell death of neural cells at different stages of differentiation. We have addressed this issue in primary cultures of differentiated hippocampal neurons and embryonic neural stem cells (NSCs). In control hippocampal neurons, pl-VDAC is closed but acts as an NADH-ferricyanide reductase, while in apoptotic neurons, pl-VDAC is opened and the enzymatic activity is increased. Anti-VDAC antibodies block pl-VDAC and prevent apoptosis, as well as the increase in enzymatic activity. Conversely, in NSCs, pl-VDAC is scarcely seen and there is no NADH-ferricyanide reductase activity. In agreement, anti-VDAC antibodies do not affect the apoptotic process. Instead, we find activation of a Na<sup>+</sup> channel that has low voltage dependency, a conductance of 26 pS, and is blocked by amiloride, which also prevents apoptosis. Thus, it appears that activation of pl-VDAC during apoptosis is a critical event in differentiated neurons, but not in NSCs.

## Introduction

Apoptosis is the best understood type of cell death occurring in the nervous system during development and pathological conditions.<sup>1</sup> One of the earliest morphological alterations occurring during the apoptotic process is the decrease in cell volume, which is associated with an increased efflux of K<sup>+</sup> and Cl<sup>-</sup> ions through ion channels in the plasma membrane.<sup>2-9</sup> The increased K<sup>+</sup> efflux leads to a reduction of the intracellular K<sup>+</sup> concentration, which facilitates the activation of caspases, cysteine proteases playing a key role in

apoptosis.<sup>9,10</sup> In line with the important role of plasma membrane ion channels, blocking of K<sup>+</sup> or Cl<sup>-</sup> channels prevents cell shrinkage and cell death.<sup>5-8</sup>

Recently, we reported that a voltage-dependent anion channel in the plasma membrane (pl-VDAC) is activated in neuronal cell lines during apoptosis.<sup>11</sup> This was based on an electrophysiological characterization and immunocytochemical identification. Block of the channel prevented the apoptotic process suggesting an essential role for this channel in apoptosis. It has also been reported that the pl-VDAC works as NADH-ferricyanide reductase to maintain redox homeostasis.<sup>12</sup> In the apoptotic cells we found a time-dependent increase in the NADH-ferricyanide reductase activity.<sup>11</sup> Thus, pl-VDAC seems to play a dual role: (1) control of redox homeostasis and (2) anion efflux in apoptotic neuronal cells.<sup>11</sup>

Whether or not VDAC is present and has a function in the plasma membrane of neural cells at different stages of differentiation is not clear yet. To address this issue, we performed the present study in primary cultures of differentiated rat hippocampal neurons, and embryonic neural stem cells (NSCs) exposed to the protein kinase inhibitor staurosporine (STS) to induce apoptosis. Interestingly, we found pl-VDAC in the hippocampal neurons, where it showed characteristics similar to those we have found in our previous investigations, using the hippocampal HT22 and the neuroblastoma SK-N-MC cell lines.<sup>11,13</sup> To our surprise, VDAC was only occasionally detected in the NSCs with no correlation to the apoptotic process. In contrast, during apoptosis NSCs activate a Na<sup>+</sup> channel absent in the hippocampal neurons. These data suggest that there are different mechanisms regulating ion flux in neurons and NSCs undergoing apoptosis.

## Results

In this investigation, we have studied primary hippocampal neurons and primary NSCs during apoptosis using electrophysiological, biochemical, and immunocytochemical methods. Apoptosis was induced by 2–12 hours treatment with 1 μM STS as previously described.<sup>11</sup> In both cell types we found an increased electrical activity during apoptosis in excised membrane patches. However, different channels were activated in the different cell types.

\*Correspondence to: Sandra Ceccatelli; Department of Neuroscience; Karolinska Institutet; Stockholm SE-171 77 Sweden; Email: Sandra.Ceccatelli@ki.se

Submitted: 08/19/08; Accepted: 08/20/08

Previously published online as a *Cell Cycle* E-publication:  
<http://www.landesbioscience.com/journals/cc/article/6831>

STS induces apoptosis and activates VDAC in the plasma membrane of primary hippocampal neurons. Hippocampal neurons exposed to STS underwent morphological changes and showed typical features of apoptosis, such as cell shrinkage and cell detachment as compared to the controls (Fig. 1A and B). In addition, at this time point (4 h), release of cytochrome *c* (cyt *c*) from the mitochondria could be observed in several cells (Fig 1C and D). However, a significant caspase activation was detected only at later time points (Fig. 1E), in agreement with our previous investigation in neuronal cell lines, where pl-VDAC was activated before caspase activation.<sup>11</sup> Figure 2A shows a voltage-clamp recording from an excised membrane patch of an apoptotic (STS-induced) neuron. The holding voltage is 0 mV and the test-step voltages are +80 mV and -80 mV respectively. The channel is open in the very beginning of the pulses and closed after about 10 ms at both voltages. Figure 2B shows the single-channel current versus voltage,  $I(V)$ , curve in excised inside-out membrane patches. The data points are collected from nine cells and are well fitted with a straight line (Eq. 2) with a reversal potential close to 0 mV. The single-channel conductance is  $372 \pm 4$  pS, which is not significantly different from the conductance in HT22-cells ( $397 \pm 12$  pS).<sup>11</sup> A characteristic feature of VDAC is a bell-shaped open-probability versus voltage,  $p_o(V)$ , curve.<sup>11,13-19</sup> To measure  $p_o(V)$  we stepped the voltage from 0 mV (where the channel is open most of the time) to either positive or negative voltages and measured the open probability after 100 ms, where the channel has reached a pseudo steady state for most of the voltages.

If longer pulses were used the channel is pushed into a long-lasting inactivated state preventing further experiments for a long time.<sup>13</sup>  $p_o(V)$  is bell-shaped, with about 80% open channels at 0 mV (Fig. 2C). The characteristics shown in Figure 2A–C are very similar to the pl-VDAC recordings from the hippocampal cell line.<sup>11,13</sup> As in our previous study, pl-VDAC is also highly activated during apoptosis. Figure 2D shows the percentage of patches with activated channels in apoptotic versus control cells. pl-VDAC is found in 30% of excised inside-out membrane patches from apoptotic cells (11/37), while there is no activation in control cells (0/20) ( $p = 0.0004$ ).

**Anti-VDAC antibodies show VDAC-like immunoreactivity, prevents apoptosis and blocks channel currents in primary hippocampal neurons.** To visualize the presence

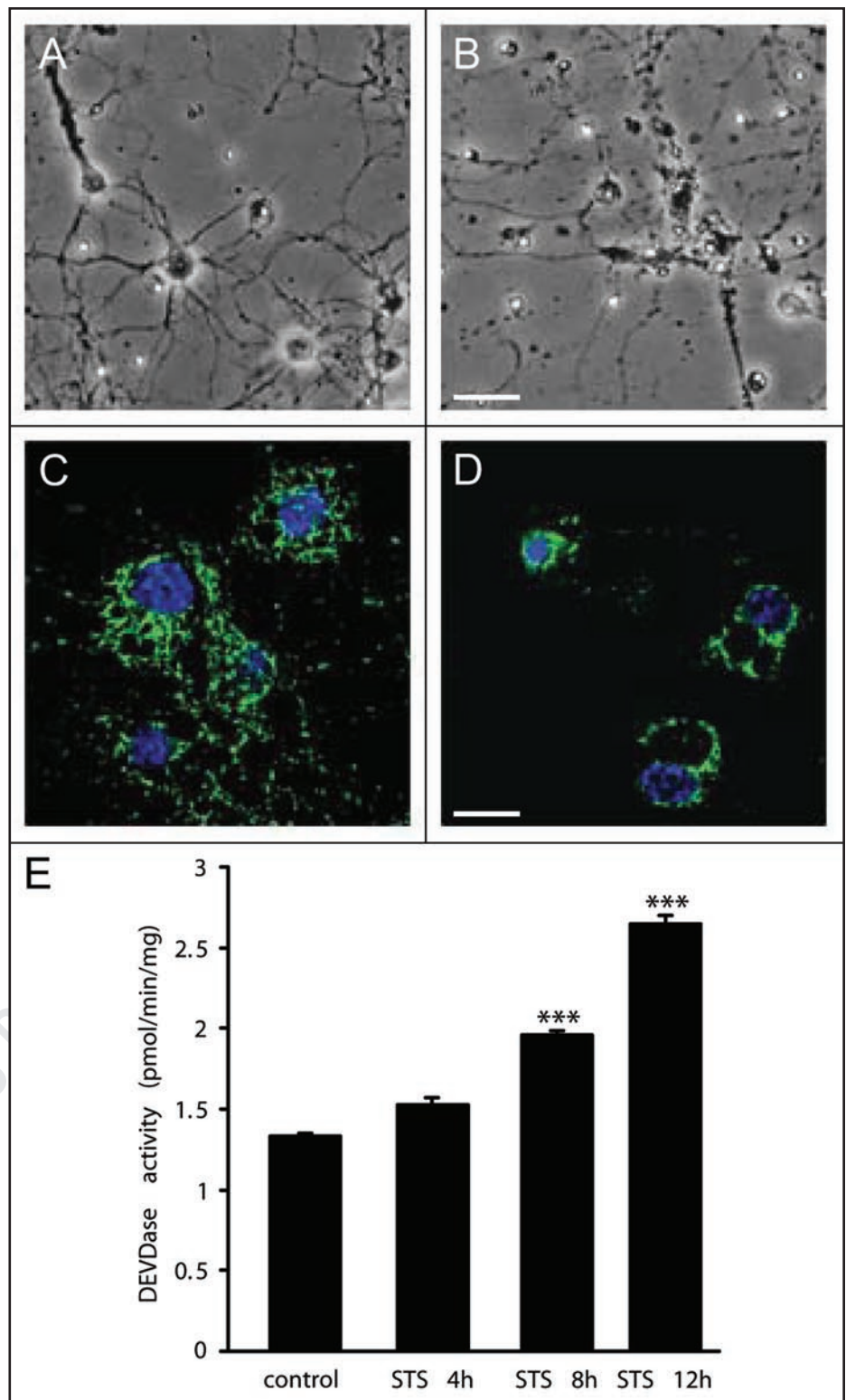


Figure 1. Typical apoptotic features induced by STS in primary hippocampal neurons. Phase contrast micrographs showing control (A) and apoptotic cells after 4 h exposure (B). Scale bar = 40  $\mu$ m. Immunofluorescence micrographs showing cyt *c* immunoreactivity in control cells (C); cells exposed for 4 h to STS show a diffuse cytoplasmic cyt *c* staining (D). Scale bar = 15  $\mu$ m. Caspase activity was measured with the fluorimetric DEVDase assay. The DEVDase activity was significantly increased only after 8 h STS-exposure (E). Values are means  $\pm$  SEM of 3 determinations. Statistical analysis was carried out with the one-way analysis of variance (ANOVA)-Fisher's protected least significant difference (PLSD) test (\*\*\*)  $p \leq 0.001$ . Cyt *c* = green, Hoechst 33358 = blue.

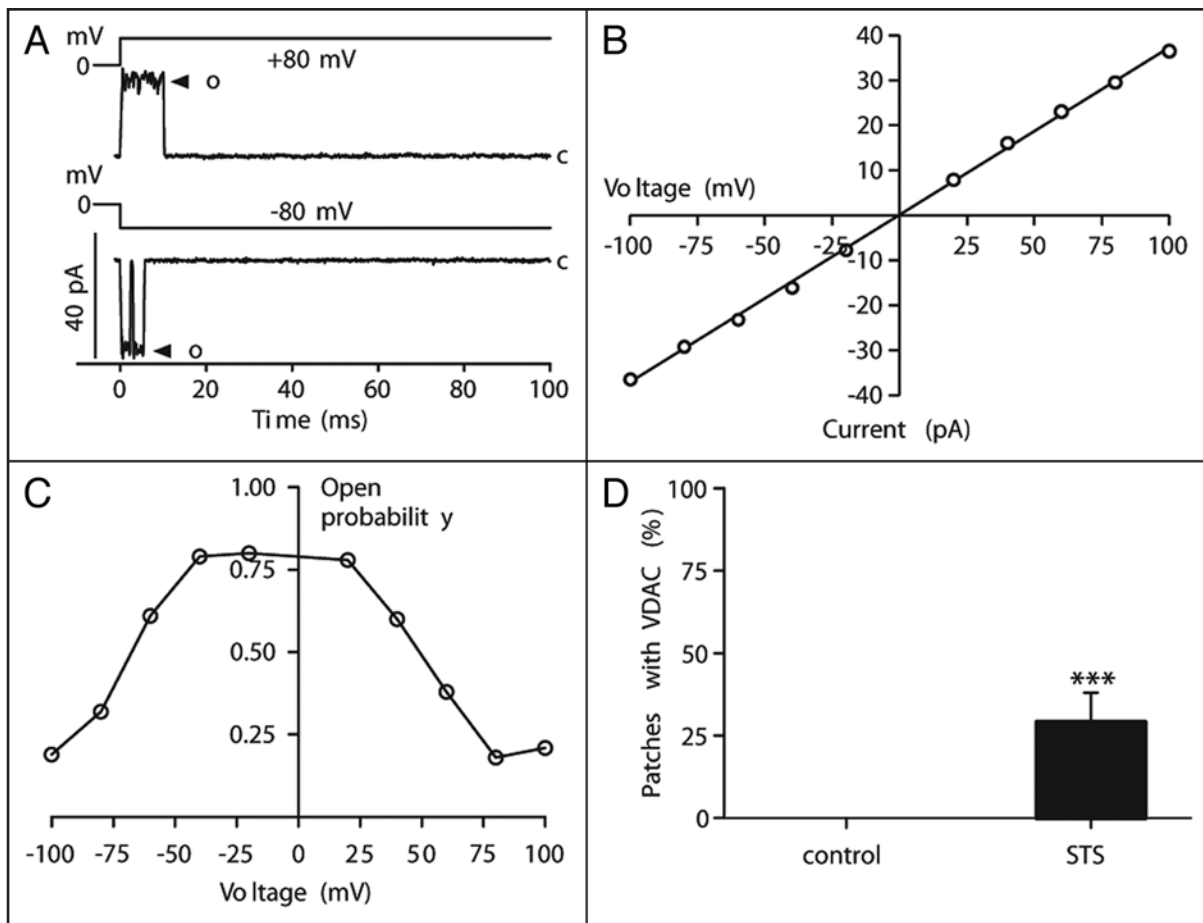


Figure 2. Electrophysiological properties of pl-VDAC in apoptotic (STS-induced) primary cultured hippocampal neurons from rat. (A) A typical voltage-clamp recording from an excised membrane patch.  $V_H = 0$  mV. Test-step voltages are +80 mV and -80 mV. O denotes open and C denotes closed channels. (B)  $I/V$  of the single-channel current. Conductance is  $372 \pm 4$  pS, and the reversal potential is 0 mV. Data points are mean  $\pm$  SEM (bars are hidden within the symbols) from three consecutive recordings from nine cells. (C) Open probability of the channel measured at the end of a 100 ms pulse.  $V_H = 0$  mV. Data points are mean  $\pm$  SEM (bars are within the symbols) from three consecutive recordings from nine cells. (D) Frequency diagram of VDAC in control and apoptotic (STS-induced) primary hippocampal neurons (inside-out patches).

of VDAC we performed immunocytochemical experiments on unpermeabilized control primary hippocampal neurons fixed with glutaraldehyde fixation. To confirm that pl-VDAC immunostaining was indeed present on the plasma membrane and not in the mitochondria due to leaking of the antibody into the cytosol, cells were prior fixation incubated with cell-permeable mitochondria-selective dye MitoTracker Red. Aldehyde-based fixatives can affect the energetic state of the mitochondria, therefore MitoTracker probes, which accumulate in active mitochondria and are well retained in fixed cells are commonly used before fixation. In addition to anti-VDAC immunostaining, cells were also co-stained with the cell-permeable DNA-selective dye Hoechst 33358. VDAC-immunoreactivity was detected on the plasma membrane of primary hippocampal neurons, and the staining was not co-localized with MitoTracker Red (Fig. 3A). To investigate the functional role of pl-VDAC during apoptosis, we pre-incubated the cells with anti-VDAC antibody for 30 min prior to exposure to STS for 4 h. Figure 3B shows the percentage of apoptotic nuclei in control versus STS-exposed cells (19%). In agreement with our previous results,<sup>11</sup> STS-treated cells pre-incubated with anti-VDAC antibodies, exhibited a significant reduction in the number of apoptotic nuclei (Fig. 3B), pointing to a critical role of pl-VDAC in neuronal apoptosis.

To explore if the antibody could block or prevent the activation of the channel, we investigated primary hippocampal neurons treated with STS in combination with the anti-VDAC antibody using the patch-clamp technique. Not a single patch from 31 investigated cells exhibited pl-VDAC currents (data not shown). This is significantly different from STS treated neurons in the absence of the antibody ( $p = 0.0004$ ).

**Ferricyanide reductase activity is increased during apoptosis in primary hippocampal neurons.** VDAC1 protein in the plasma membrane functions as NADH-ferricyanide reductase, which is involved in transmembrane redox regulation.<sup>12</sup> In our previous investigation we also found that during apoptosis, in addition to the activated pl-VDAC, there was an increased NADH-ferricyanide reductase activity, suggesting a dual role for pl-VDAC.<sup>11</sup> To further corroborate our hypothesis, we performed experiments in primary hippocampal neurons. Figure 4 shows that the NADH-ferricyanide reductase activity was significantly increased in the STS-exposed primary hippocampal neurons and that pre-incubation with anti-VDAC antibodies significantly decreased the enzyme activity.

**STS induces apoptosis without activating pl-VDAC in primary cultures of NSCs.** Primary NSCs were exposed for 4 h to the same concentration of STS as the primary hippocampal neurons. Like

STS-exposed primary hippocampal neurons, exposed NSCs also exhibited morphological changes, such as cell shrinkage and cell detachment, compared to the control cells (Fig. 5A and B). Release of cyt *c* from the mitochondria started to be detectable after 4 h exposure (not shown), and increased with time (Fig. 5D). Activation of caspases, as detected by using an antibody against the active fragment of caspase 3, was observed after 8 h exposure (Fig. 5D).

In contrast to the cell lines<sup>11,13</sup> and the primary hippocampal neurons (present investigation), pl-VDAC was not activated during apoptosis in NSCs. pl-VDAC or pl-VDAC-like channels were only found in 3 patches taken from 179 cells. One of them was found in a control cell (1/58) and two of them in apoptotic cells (2/121). Furthermore, two of them showed atypical voltage dependencies. Figure 6A shows a recording of an atypical VDAC in the plasma membrane of apoptotic (STS-induced) NSCs. The holding voltage is 0 mV and the test-step voltages are +100 mV and -100 mV respectively. At +100 mV the channel is open for the entire pulse length (100 ms), while at -100 mV the channel closes after about 40 ms. The conductance of this channel is  $418 \pm 4$  pS. In contrast to the bell-shaped  $p_O(V)$  curve of a normal pl-VDAC, the present  $p_O(V)$  curve is sigmoidal (Fig. 6B; measured as for the primary hippocampal neurons above). Figure 6C shows the current for another atypical pl-VDAC. The holding voltage is 0 mV and the test-step voltages are +100 mV and -100 mV respectively. At +100 mV the channel is open at the beginning of the pulse and at the end of the pulse with a closure in between; while at -100 mV the channel is closed for the entire pulse length (100 ms). The conductance of this channel is  $352 \pm 26$  pS. The  $p_O(V)$  curve is also here sigmoidal (Fig. 6D) instead of being bell shaped. However, the  $p_O(V)$  curve is shifted about 100 mV in positive direction along the voltage axis compared to the channel in Figure 6A. The third example of VDAC in NSCs was found in a control cell and showed typical pl-VDAC characteristics (data not shown) as we have reported before.

In line with relative absence of electrophysiologically verified pl-VDAC, preincubation of NSCs with the anti-VDAC antibodies before STS treatment had no protective effect against apoptosis, and no NADH-ferricyanide reductase activity was found in the NSCs (data not shown).

**An amiloride sensitive  $\text{Na}^+$  channel is activated in the plasma membrane of NSCs during apoptosis.** In contrast to the lack of VDAC activation, we found another ion channel significantly activated in NSCs undergoing apoptosis. This channel was not seen in the primary hippocampal neurons. Figure 7A shows a voltage-clamp recording of an excised membrane patch from an apoptotic (STS-induced) NSC. The holding voltage is 0 mV and the test-step voltage is to -100 mV. Initially four or possibly five channels are seen. The open probability is changing during the pulse, and two channels are open after 100 ms. The time constant for the current decay is approximately 20 ms (dashed line). All channel openings have the same amplitude (see amplitude histogram in Fig. 7B) suggesting that only one type of channels is seen. The activation of this channel is increased three fold during apoptosis (Fig. 7C;  $p = 0.0002$ ). The channel is found in 44% (53/121) of excised membrane patches from apoptotic cells, while, it is found in only 16% (9/58) of control cells.

To further characterize the channel we measured the single-channel conductance, the voltage dependence of the open probability, and the selectivity. Figure 7D shows the  $I(V)$  of the single-channel currents in

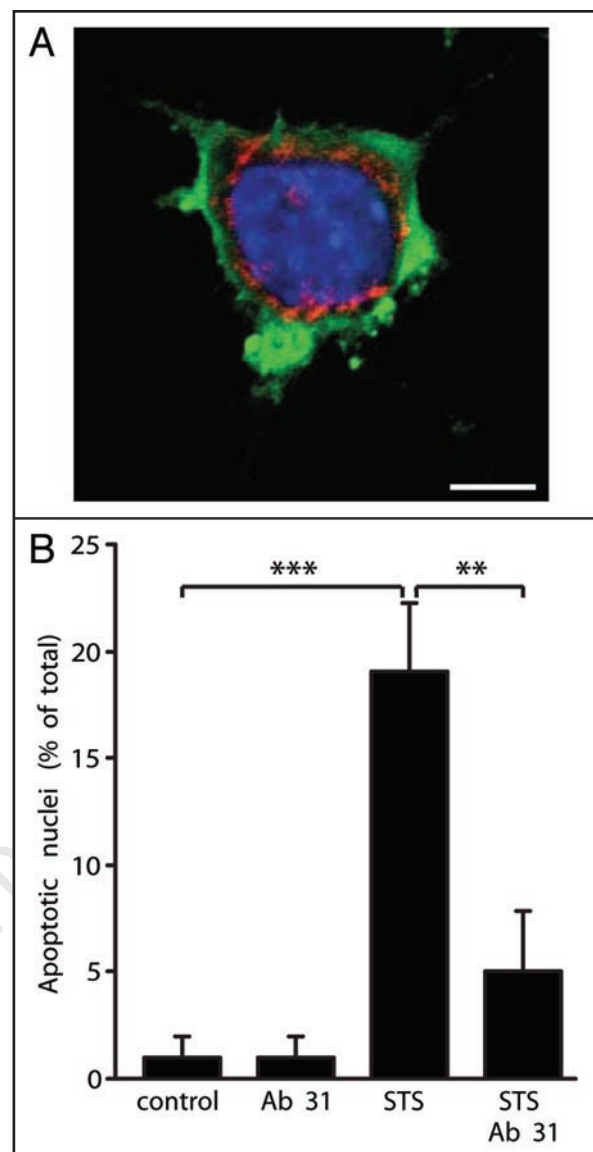


Figure 3. Presence of VDAC on the plasma membrane of primary hippocampal neurons and prevention of apoptosis by VDAC antibodies. (A) shows representative staining of a hippocampal cell incubated with the mitochondria selective dye Mitotracker Red, fixed with glutaraldehyde and stained with anti-VDAC antibodies (anti-Porin 31 HL = ab 31). The cell was also co-stained with the DNA-selective dye Hoechst 33358. Scale bar = 7.5  $\mu\text{m}$ . (B) Cells fixed with methanol were stained with Hoechst 33358 and the nuclei were scored at the fluorescence microscope. Preincubation of primary hippocampal neurons with the same VDAC antibodies for 30 min prior to exposure to 1  $\mu\text{M}$  STS (4 h), significantly reduced the number of apoptotic nuclei. Values are means  $\pm$  SEM of 8 determinations. Statistical analysis was carried out with the one-way analysis of variance (ANOVA)-Fisher's protected least significant difference (PLSD) test (\*\* $p \leq 0.01$  and \*\*\* $p \leq 0.001$ ). pl-VDAC = green, Mitotracker Red = red, Hoechst 33358 = blue.

an inside-out membrane patch. The data points are well fitted with a straight line (Eq. 2) with a reversal potential close to 0 mV and a slope of 25 pS. The mean value is  $26.4 \pm 1.0$  pS ( $n = 5$ ). As seen in Figure 7A, the channel is slightly voltage dependent with a lower open probability at negative voltages. Data from 24 current families in five cells is collected in Figure 7E. A Boltzmann curve (Eq. 3) is fitted to the data. The midpoint  $V_{1/2}$  is +37 mV and the slope  $s$  is 80 mV. The main charge-carrying ions in the symmetrical extracellular

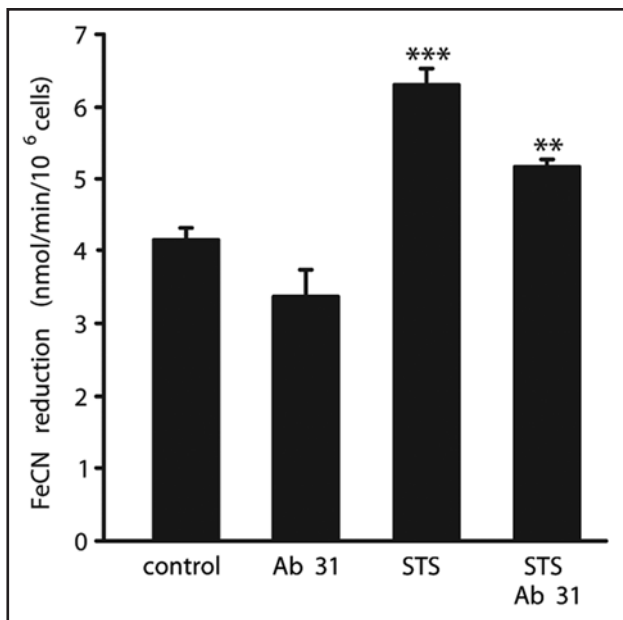


Figure 4. Increased NADH-ferricyanide reductase activity during apoptosis. Primary hippocampal neurons exposed to 1  $\mu$ M STS for 4 h showed significant increase in NADH-ferricyanide reductase activity, while pre-incubation with anti-VDAC antibodies (anti-Porin 31 HL = ab 31) for 30 min prior to exposure to STS decreased significantly the activity of the enzyme. Values are means  $\pm$  SEM of 3 determinations. Statistical analysis was carried out with the one-way analysis of variance (ANOVA)-Fisher's protected least significant difference (PLSD) test (\*\* $p \leq 0.01$  and \*\*\* $p \leq 0.001$ ).

solutions are Na<sup>+</sup> and Cl<sup>-</sup>. To explore the selectivity of the channel we diluted the bath solution five times. Based on Nernst's equation we expected the reversal potential to shift -41 mV for a Cl<sup>-</sup>-selective channel and +41 mV for a Na<sup>+</sup>-selective channel. Figure 7F shows recordings at 0 mV and at -80 mV. In control solution no current is seen at 0 mV, because of the symmetrical solutions. An inward-going current is seen when the membrane voltage is changed to -80 mV (lower). When the bath solution is diluted to 1/5, an inward going current is clearly seen at 0 mV. The channel is open in the beginning and the end of the trace but make a spontaneous closure in the middle. This suggests that the current is carried by Na<sup>+</sup>. In the lower panel, the channel is open in the beginning of the trace (at 0 mV, before the test pulse). When the membrane voltage is changed to -80 mV the current increases instantaneously, because of the increased driving force. Later in the pulse, the channel closes. Figure 7G shows an I(V) plot from this cell showing that the reversal potential is shifted +37 mV, thus close to the expected +41 mV for a pure Na<sup>+</sup> selective channel. Data from two other cells also give values between +30 and +40 mV.

**The epithelial Na<sup>+</sup> channel blocker amiloride prevents apoptosis in neural stem cells but not in hippocampal neurons.** What is the identity of the Na<sup>+</sup> channel activated during apoptosis in NSCs? There are two general types of Na<sup>+</sup> selective channels: (1) Classical Na<sup>+</sup> channels with six transmembrane spanning segments per domain (Nav). These channels are found in excitable tissues, they are voltage dependent, most of them are only transiently open, and most of them are also highly sensitive to the puffer-fish toxin tetrodotoxin (TTX). (2) Another type of Na<sup>+</sup> channel has two transmembrane spanning segments per subunit and constitutes the

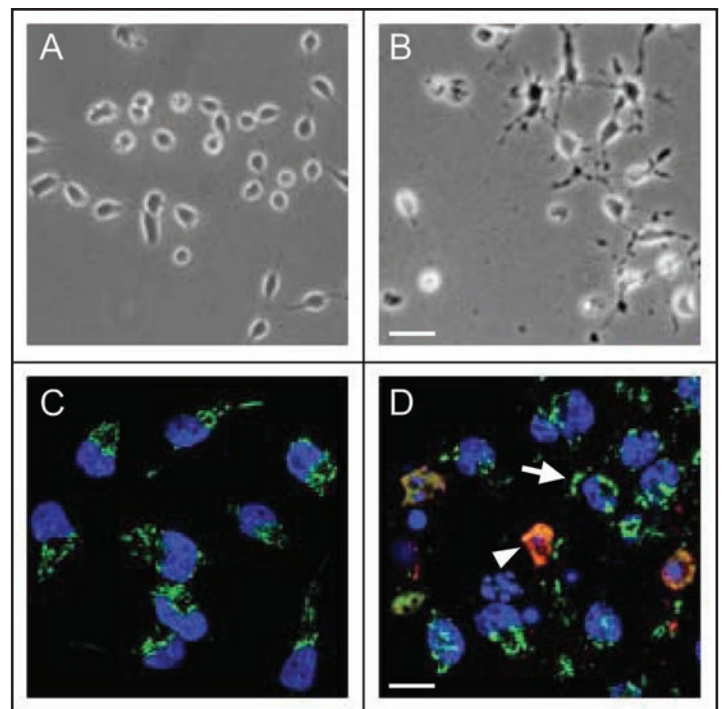


Figure 5. Induction of apoptosis in primary cultures of NSCs. (A) Phase contrast micrographs showing control primary NSCs and (B) detached and condensed apoptotic cells after 4 h exposure to STS. Scale bar, 20  $\mu$ m. Immunofluorescence micrographs showing control (C) and STS-exposed cells after 8 h (D). Scale bar, 10  $\mu$ m. In control cells cyt c immunoreactivity was detected in the mitochondria, while in STS-exposed cells cyt c staining was diffused into the cytoplasm (arrow), and presence of the active fragment of caspase 3 was detected in few cells (arrowhead). Cyt c, green; caspase 3, red; Hoechst 33358, blue.

epithelial Na<sup>+</sup> channel/degenerin (ENaC/DEG) family.<sup>20,21</sup> They are all voltage-independent Na<sup>+</sup> channels and they are blocked by low concentrations of the diuretic drug amiloride. The two channel types are not molecularly related. The single-channel conductance of 26 pS found in the present investigation fits with most Nav channels<sup>22</sup> but it also fits with some of the ENaC/DEG channels, even though most of them have conductances between 5 and 15 pS.<sup>20,21</sup> The low voltage dependence including the persistent opening fits better with ENaC/DEG than with the highly voltage dependent and (in most cases) transiently open Nav channels. To pharmacologically test the identity of the channel we performed experiments with either 1  $\mu$ M TTX or with 10  $\mu$ M amiloride in the pipette solution of excised membrane patches. Amiloride but not TTX blocked the apoptosis-induced channel (Fig. 7H), suggesting that the channel activated during apoptosis belongs to the ENaC/DEG family.

To explore whether the increased activation of amiloride-sensitive Na<sup>+</sup> channels, plays a role in the apoptotic process in NSCs, we tried the effect of 10  $\mu$ M amiloride on NSCs exposed to 1  $\mu$ M STS for 4 h. Amiloride markedly reduced apoptosis (Fig 8). No protective effect on hippocampal neurons were detected with amiloride after exposure to STS for 4 h (data not shown).

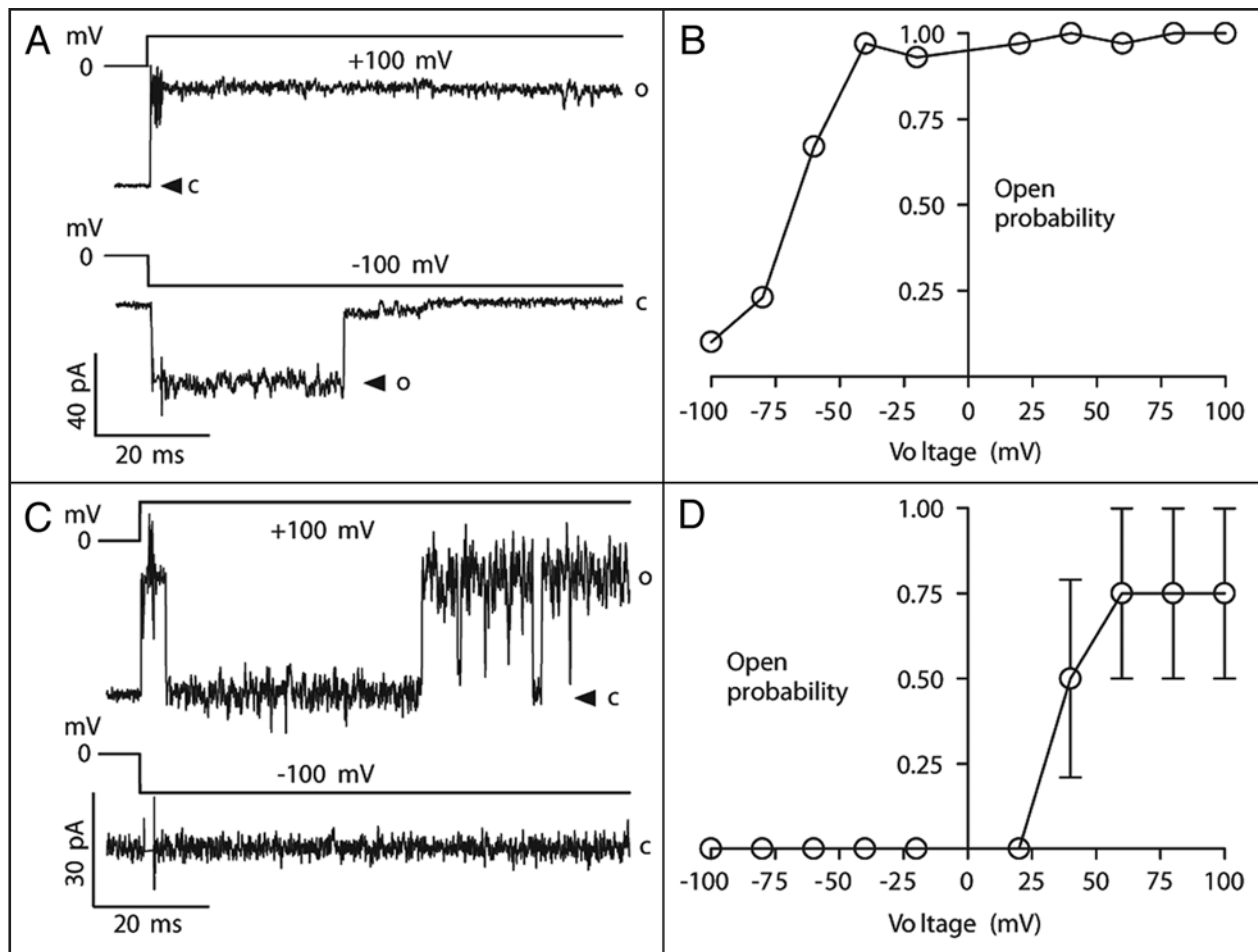


Figure 6. VDAC in the plasma membrane of apoptotic (STS-induced) primary cultured rat NSCs. (A) A voltage-clamp recording from an excised membrane patch,  $V_H = 0$  mV. Test-step voltages are +100 mV and -100 mV. O denotes open state and C denotes close states. (B) Open probability of the channel measured at the end of a 100 ms pulse.  $V_H = 0$  mV. Data points are mean  $\pm$  SEM values (bars are hidden within the symbols) from 30 consecutive recordings from one cell. (C) A voltage-clamp recording from an excised membrane patch from another cell.  $V_H = 0$  mV. Test-step voltages are +100 mV and -100 mV. (D) Open probability of the channel measured at the end of a 100 ms pulse.  $V_H = 0$  mV. Data points are mean  $\pm$  SEM values from four consecutive recordings from one cell.

## Discussion

In this investigation, we have searched for pl-VDAC and its role in apoptosis, in two different neural cell types: hippocampal neurons and embryonic neural stem cells (NSCs). In the differentiated hippocampal neurons, the activation of pl-VDAC is dramatically increased during apoptosis. In contrast, pl-VDAC is sporadically seen in only a few control, or apoptotic NSCs. Instead an amiloride-sensitive  $\text{Na}^+$  channel is shown to play a critical role for apoptosis in NSCs. Table 1 summarizes the experimental findings presented in this investigation.

**PI-VDAC changes during development.** In differentiated hippocampal neurons, pl-VDAC plays a similar role as we have reported for the hippocampal and neuroblastoma cell lines.<sup>11</sup> The channel is significantly activated in apoptotic cells, and block of pl-VDAC prevents apoptosis. In contrast to this scenario, activation of pl-VDAC is hardly seen in the NSCs. Thus, our data suggest that pl-VDAC gains a critical role in apoptosis during neuronal differentiation. An interesting observation in relation to this development is that pl-VDAC in two of the three recordings from NSCs showed an atypical behaviour: the channel had a sigmoidal voltage dependence,

being open at positive voltages, in contrast to the bell-shaped voltage dependence normally seen.<sup>11,13</sup> We speculate that this gating behavior depends on an immature channel protein with only one of two hypothetical gates working properly.

**Is pl-VDAC identical to mitochondrial VDAC?** VDAC was originally reported in the outer membrane of the mitochondrion,<sup>23</sup> where it plays a role in early stages of certain forms of apoptotic cell death.<sup>14,24</sup> Later on a VDAC-like protein was shown to exist in the plasmamembrane (thus pl-VDAC).<sup>15</sup> Since then, the presence of VDAC in the plasma membrane has been heatedly debated.

In our previous studies, we demonstrated the presence of VDAC in the plasma membrane as well as in the mitochondria of HT22 cells by immunocytochemistry using three different anti-VDAC antibodies.<sup>11</sup> Further, we showed that the electrophysiological characteristics are almost identical for mitochondrial VDAC and for pl-VDAC.<sup>13</sup> In the present study, we found that the antibody anti-Porin 31 HL Ab-2, which also recognized mitochondrial VDAC, showed similar VDAC-like immunoreactivity in the plasma membrane of unpermeabilized primary hippocampal neurons. In our immunocytochemical experiments, pl-VDACs were detected both in control and apoptotic cells, suggesting that the channels are

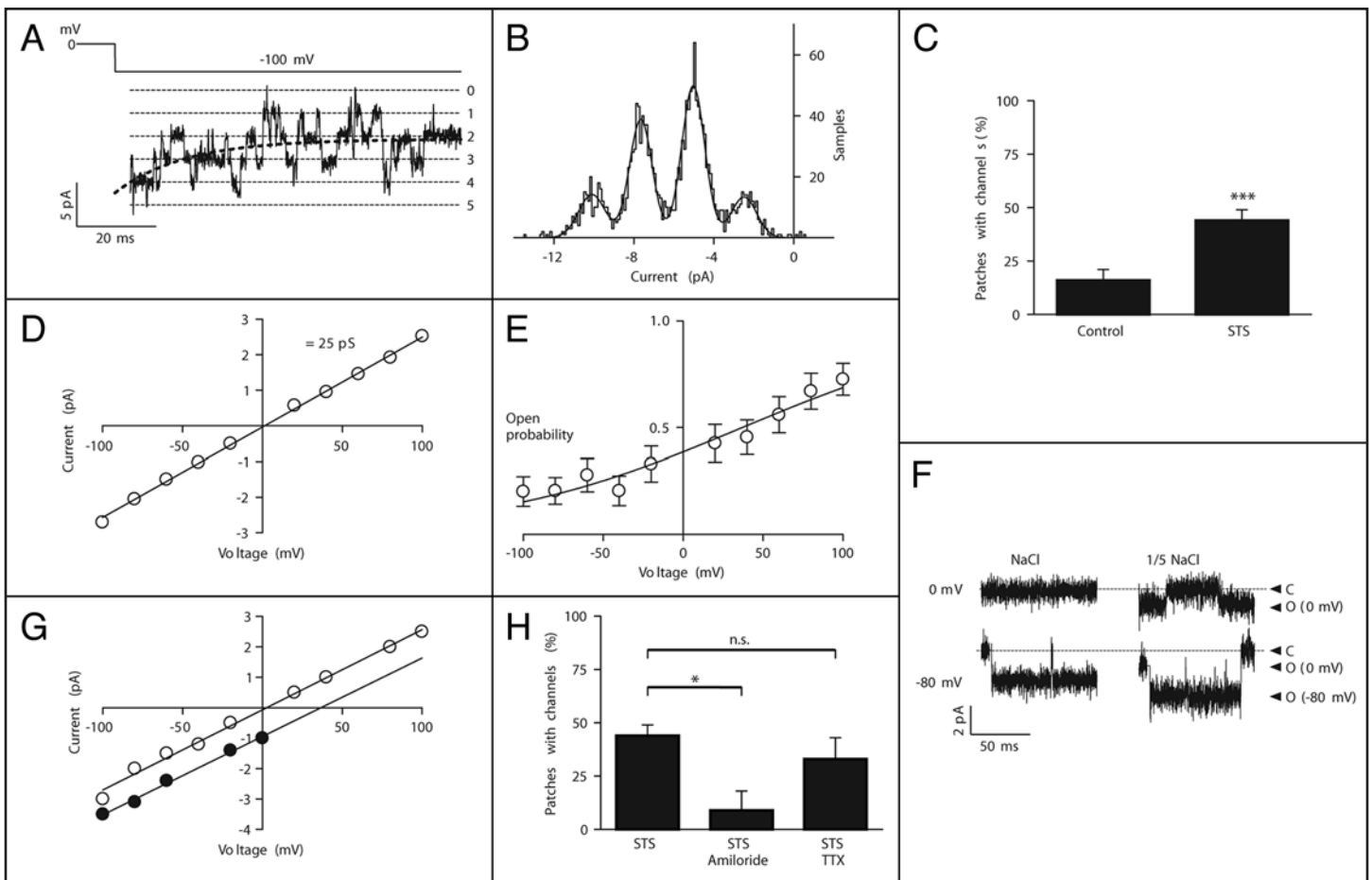


Figure 7. A  $\text{Na}^+$  channel activated during apoptosis in primary cultured NSCs. (A) Voltage-clamp recording from an excised membrane patch.  $V_H = 0$  mV. Test-step voltage is  $-100$  mV. Thin dashed lines denote current levels separated by  $2.5$  pA. 0, 1, 2, 3, 4 and 5 denote the number of open channels. Thick dashed line is a least-square fitted exponential relaxation with a time constant of  $18$  ms. (B) Amplitude histogram of single-channel currents from (A). Bin width =  $0.1$  pA. The histogram was fitted to the sum of four Gaussian curves (Eq. 1 in Methods). All units in pA.  $A_1 = 21.1$ ,  $i_1 = -2.48$ ,  $s_1 = 0.63$ ,  $A_2 = 72.1$ ,  $i_2 = -5.03$ ,  $s_2 = 0.58$ ,  $A_3 = 55.2$ ,  $i_3 = -7.65$ ,  $s_3 = 0.57$ ,  $A_4 = 23.7$ ,  $i_4 = -10.09$ ,  $s_4 = 0.67$ . (C) Frequency diagram of the channel in excised inside-out patches from control and apoptotic (STS-induced) NSCs. \*\*\* Significantly different than control ( $p \leq 0.001$ ). (D)  $I/V$  of the single channels current. Conductance is  $25.3$  pS, and the reversal potential is  $+1.4$  mV (not significantly different from 0; Eq. 2). Data points are mean  $\pm$  SEM values from 4–9 determinations. (E) Open probability of the channel measured at the end of a  $100$  ms pulse. Midpoint voltage  $V_{1/2} = 37$  mV, and slope factor  $s = 80$  mV (Eq. 3). Data points are mean  $\pm$  SEM values from 24 determinations from 5 cells. (F) Single-channel recordings of excised patches at  $0$  mV and  $-80$  mV in symmetrical extracellular solutions (left) and in asymmetrical solutions (right; control extracellular solution in pipette, and  $1/5$  control solution in bath). Membrane voltage is  $0$  mV during the first  $10$  ms in each recording. C denotes closed state and O open state. (G)  $I/V$  curves from recordings of the type in (F). Open symbols denote control and closed symbols  $1/5$  control solution.  $V_{\text{rev}}$  in  $1/5$  is  $+37$  mV. (H) Frequency diagram of the channel in excised inside-out patches for STS-treated cells in combinations with the channel blockers amiloride and TTX. \* Significantly different from STS ( $p < 0.05$ ).

constitutively present in the plasma membrane, but activated only during apoptosis.

Based upon their biophysical similarities, pl-VDAC and the maxi-anion channel, have been considered for a long time to be the same channel. This has been supported by common properties such as the large conductance, a bell-shaped voltage dependency;<sup>11,25</sup> similar size of inner pore radius<sup>26,27</sup> and conductivity of ATP.<sup>28,29</sup> However, Sabirov et al.,<sup>30</sup> have shown that deletion and/or silencing of the VDAC genes in the fibroblasts do not eliminate the channel activity nor abolish the maxi-anion channel-mediated ATP release. Therefore, they concluded that the maxi-anion channel is not encoded by VDAC genes and the two channels are unrelated proteins. Nevertheless, they do not exclude the fact that VDAC proteins can be targeted to the plasma membrane and exert other functions, such as a trans-plasma membrane NADH (-ferricyanide) reductase. This is in agreement

with our previous and present results, where we found NADH (-ferricyanide) reductase activity in normal and apoptotic neurons. However, according to our findings, VDAC protein can besides acting as an enzyme, also function as an anion channel activated only in apoptotic neurons. In line with our results, the presence of VDAC in the plasma membrane of hippocampal HT22 and septal SN56 neurons was demonstrated in a recent study by Marin et al.<sup>31</sup> The authors also showed that anti-VDAC antibodies protect hippocampal and septal neurons against amyloid beta ( $\text{A}\beta$ ) peptide-induced neurotoxicity and suggested that VDAC at the plasma membrane level may participate in the modulation of  $\text{A}\beta$ -induced cell death.

In contrast to hippocampal neurons, NSCs do scarcely express VDAC as shown by our electrophysiological, immunocytochemical and biochemical results. While blocking of pl-VDAC with an anti-

VDAC antibody 30 min prior STS exposure prevented apoptosis in primary hippocampal neurons, the same antibody had no protective effect on STS-exposed NSCs. All together these results point to the occurrence of functional pl-VDACs only in apoptotic differentiated neurons, while apoptotic NSCs lack this channel activity.

**Amiloride-sensitive Na<sup>+</sup> channel involved in apoptosis of neural stem cells.** The absence of pl-VDAC activation during apoptosis in the undifferentiated NSCs leads to the hypothesis of an alternative mechanism. Our electrophysiological experiments showed that a Na<sup>+</sup> channel sensitive to amiloride but not TTX, is activated during apoptosis in NSCs. In agreement, pre-incubation with amiloride prevented apoptosis of NSCs exposed to STS for 4 h, suggesting a crucial role for the amiloride-sensitive channel in the apoptotic process. It is unlikely that this protective effect depends on an unselective channel block, because much higher concentrations are needed to block Ca<sup>2+</sup> channels.<sup>21</sup>

Amiloride-sensitive Na<sup>+</sup> channels are normally found in the epithelium lining the distal part of kidney tubule, the urinary bladder and the distal colon, where they are involved in sodium reabsorption. The epithelial Na<sup>+</sup> channel (ENaC) belongs to a channel family with voltage-independent and amiloride sensitive Na<sup>+</sup> channels (ENaC/DEG), also including the degenerins from *Caenorhabditis elegans* (e.g., DEG-1 and MEC-4), the acid sensing channels (ASICs), the FMRamide-gated channel (FaNaC), and a few other channels.<sup>21,32,33</sup> Notably, mutated degenerins are involved in neuronal degeneration.<sup>34-36</sup> The current idea is that the degenerins are ion channels and that the mutations causing neurodegeneration result in gain-of-function of the putative cation channel. This prompts us to speculate, that apoptosis and neurodegeneration can be caused either by an activation of VDAC, as supported by the present and previous studies,<sup>11,31</sup> or by a gain-of-function mutation in amiloride-sensitive ion channels.

## Materials and Methods

Animals were handled according to Karolinska Institutet's and Linköpings Universitet's guidelines and experiments were performed with permission from the local ethical committees.

**Primary hippocampal cell culture.** Sprague-Dawley rats (B&K Universal AB, Sollentuna, Sweden), kept under standard laboratory conditions, were sacrificed on the 18<sup>th</sup> gestational day using carbon dioxide, and the hippocampi were dissected from the foetuses. Briefly, the cultures were prepared as follow; the dissected hippocampi were incubated at 37°C for 15 min in 0.1% trypsin (Invitrogen) diluted in Ca<sup>2+</sup>-Mg<sup>2+</sup>-free Hank's Balanced Salt Solution (pH 7.3) and subsequently triturated through a narrowed Pasteur pipette. Cell suspensions were then seeded into 35-mm tissue culture dishes (Corning, New York, NY, USA) at a cell density of 0.17 x 10<sup>5</sup> cells/cm<sup>2</sup>. Prior to seeding, the dishes were coated with 0.1 mg/ml poly-L-lysine hydrobromide (MW 3-7 x 10<sup>4</sup>; Sigma, Chemical Co., St. Louis, MO, USA) and subsequently washed twice in distilled water. The cells were grown in 2 ml Neurobasal medium and were supplemented with B27, 1:50, (NB B27), 15 µg/ml gentamicin and 2 mM L-glutamine (all from Invitrogen). The cultures were maintained in an incubator providing 5% CO<sub>2</sub> at 37°C. The growth medium was never changed and no re-feeding was done during the experimental period.

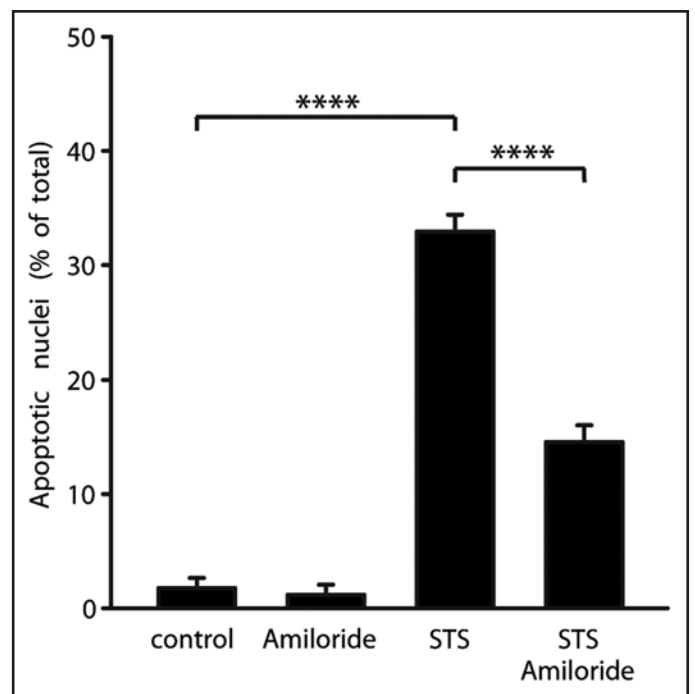


Figure 8. Prevention of apoptosis in NSCs. Preincubation of NSCs with 10 µM amiloride for 10 min prior to exposure to 1 µM STS (for 4 h), significantly reduced the number of apoptotic nuclei. Values are means ± SEM of 8 determinations. Statistical analysis was carried out with the one-way analysis of variance (ANOVA)-Fisher's protected least significant difference (PLSD) test (\*\*\*\*p ≤ 0.0001).

Table 1 Summary of the experimental findings

	Hippocampal neurons	NSCs
<b>pl-VDAC</b>		
Electrophysiology (e.g., 400 pS)	y	-
Anti-VDAC ab labels the plasmamembrane	y	-
Anti-VDAC ab blocks the channel	y	n/a
Anti-VDAC ab prevents apoptosis	y	-
<b>NADH-Ferricyanide reductase</b>		
Enzymatic activity is present in control cells	y	-
Apoptosis increases enzymatic activity	y	-
Anti-VDAC ab prevents the increase	y	n/a
<b>Amiloride-sensitive Na<sup>+</sup> channel</b>		
Electrophysiology (e.g., 26 pS)	-	y
Amiloride blocks the channel	n/a	y
Amiloride prevents apoptosis	-	y

y indicates that experimental data for a certain feature is found, and - indicates that it is not found. n/a, not applicable. See text for details.

**Primary embryonic neural stem cells.** Primary cultures of neural stem cells were obtained from embryonic cortices dissected in Hanks' Balanced Salt Solution (HBSS) (Life Technologies) from timed-pregnant Sprague-Dawley rats (B&K, Sollentuna, Sweden) at E15 (E1 was defined as the day of copulatory plug). The tissue was gently mechanically dispersed, and meninges and larger cell clumps were

allowed to sediment for 10 min. The cells were plated at a density of  $0.6 \times 10^6$  cells per 100-mm cell culture dish precoated with poly-L-ornithine and fibronectin (both from Sigma). Cells were maintained in enriched N2 medium<sup>37</sup> with 10 ng/ml basic fibroblast growth factor (bFGF) (R&D Systems, Minneapolis, MN, USA) added every 24 h and the medium changed every other day to keep cells in an undifferentiated and proliferative state. When still subconfluent, cells were passaged by incubation with HBSS and subsequent scraping to detach the cells. Afterwards, the cells were gently mixed in N2 medium, counted and plated at the desired density. The cells were used for experiments 48 h after the first passage. At the time of experiments all cells were nestin positive, confirming their proliferative and undifferentiated status.

**Induction, prevention and evaluation of apoptosis.** To induce apoptosis, cells were exposed to the protein kinase inhibitor staurosporine (STS; 1  $\mu$ M) for 2 to 12 hours. To prevent apoptosis, cells were pre-incubated for 30 min with anti-VDAC antibody anti-Porin 31 HL Ab-2 (Calbiochem) (1:100) or for 10 min with 10  $\mu$ M amiloride (Sigma). For control purpose two other VDAC antibodies raised against different epitopes were used in some of the experiments (data not shown).<sup>11</sup> The occurrence of apoptosis was evaluated on fixed cells. Cells grown on coverslips, were fixed with ice-cold methanol/water (8/2 = v/v), and stained with cell-permeable Hoechst 33358 to visualize nuclear condensation. The coverslips were mounted onto glass slides with PBS/glycerol (1/9 = v/v) containing 0.1% (w/v) phenyldiamine. Apoptotic nuclei were identified by the smaller size of the nucleus, irregular shape and brighter intensity of the stained chromatin. The percentage of nuclei with chromatin condensation was determined by scoring at least 100 nuclei in four fields on each coverslip examined, using an Olympus BX60 fluorescence microscope (Olympus, Tokyo, Japan) equipped with a C4742-95-10sc digital camera (Hamamatsu Photomics Norden AB).

**Caspase-3-like activity.** Caspase activity was measured by using a fluorogenic assay which evaluates the activity of class II caspases (caspase 2, 3 and 7), a method which has been previously described<sup>38</sup> with some modifications.<sup>39</sup> Substrate cleavage leading to the release of free 4-methyl-coumaryl-7 amide (excitation 355 nm, emission 460 nm) was monitored at 37°C using a Fluoroscan II (Labsystem AB, Stockholm, Sweden). Fluorescence units were converted to pmoles of 4-methyl-coumaryl-7 amide release using a standard curve generated with 4-methyl-coumaryl-7 amide and subsequently related to protein content.

**Immunocytochemistry.** Cells were fixed with 4% paraformaldehyde (Sigma) for 60 min 4°C and then washed with PBS. Primary antibodies were diluted in PBS with 0.3% Triton-X100 and 0.5% BSA (Boehringer Mannheim, Bromma, Sweden). The following primary antibodies were used: mouse anti-cytochrome *c* (1:100) (BD Biosciences, Stockholm, Sweden), rabbit anti-active caspase 3 (p17) (1:50) (Cell signaling Technology, Beverly, MA, USA). Cells were incubated in a humid chamber at 4°C overnight, rinsed with PBS and incubated with secondary antibodies Alexa Fluor 488 and Alexa Fluor 594 respectively (Molecular Probes) (1:200) for 60 min at room temperature (RT). Cells were further incubated with Hoechst 33358 for 5 min before coverslips were mounted onto glass slides with PBS/glycerol (1/9 = v/v) containing 0.1% (w/v) phenyldiamine. Cells were analyzed with a Zeiss LSM 510 Meta confocal microscope (Zeiss, Jena, Germany).

To detect the presence of pl-VDAC, living cells were pre-incubated with 100 nM MitoTracker Red (Molecular Probes) for 30 min at 37°C. Cells were then fixed under unpermeabilized conditions in PBS (pH 7.4), containing 2% paraformaldehyde, 1% glutaraldehyde and 120 mM sucrose for 1 h at 4°C. This fixation is known to preserve plasma membrane integrity and thereby avoiding intracellular antibody leaking.<sup>40</sup> Unpermeabilized fixed cells were washed in PBS and incubated with 50 mM ammonium chloride for 1 h at room temperature to reduce the generation of free aldehyde groups. Fixed cells were then washed again in PBS and incubated overnight at 4°C with mouse anti-VDAC antibody, (anti-Porin 31 HL Ab-2) (1:100 in PBS and supplemented with 0.5% BSA). After several washes with PBS, the secondary antibody Alexa Fluor 488 (Molecular Probes) (1:200) was added for 1 h at RT. Cells were further incubated with Hoechst 33358 for 5 min and were mounted and examined as mentioned above. For control purpose, cells were also incubated with the secondary antibody alone.

**NADH-ferricyanide reductase activity.** Cells ( $1.5 \times 10^6$ ) were harvested and incubated in 1 ml buffer, containing 50 mM Tris-HCl, pH 8.0 and 250  $\mu$ M  $\beta$ -NADH for 5 min at 37°C. The reaction was started by addition of 250  $\mu$ M potassium ferricyanide to the reaction buffer leading to reduction of ferricyanide to ferrocyanide. After 10 min, cells were spun down and the concentration of remaining ferricyanide was assessed, using a UNICAM 5625 spectrophotometer, at 420 nm. Ferricyanide reductase activity was calculated as nmol ferricyanide reduced per min per  $10^6$  cells.

**Electrophysiology.** The electrophysiological recordings were done with the patch-clamp technique on control and STS-exposed cells exhibiting apoptotic morphology. We used an EPC-7 patch-clamp amplifier (HEKA Electronics, Lambrecht/Pfalz, Germany), or Axopatch 200B (Axon Instruments, Foster City, CA, USA), and pClamp software (Axon Instruments, Foster City, CA, USA). The extracellular solution was composed of (in mM): 140 NaCl, 5 KCl, 1.8 CaCl<sub>2</sub>, 1 MgCl<sub>2</sub>, 10 HEPES and 23 sucrose (pH 7.4). Amiloride and tetrodotoxin (TTX) were purchased from Sigma-Aldrich Sweden AB (Stockholm, Sweden). The patch pipettes were made of borosilicate glass and the pipette resistance was 4–6 M $\Omega$  with the extracellular solution. We used the extracellular solution in the bath. We also tried an intracellular solution on the intracellular side of inside-out patches in our previous report, but no difference was seen regarding VDAC activity.<sup>11</sup> The current was always denoted as positive for currents from the intracellular side towards the extracellular pipette side and the membrane voltage is defined as bath voltage minus pipette voltage. The normal pulse protocol consisted of 100 ms pulses to voltages between -100 and +100 mV in steps of 20 mV. The holding voltage,  $V_H$ , was 0 mV and the time between the pulses was 400 ms. All recordings were carried out at room temperature (20–22°C). The sampling frequency was 10 kHz and the signal was filtered at 5 kHz.

**Analysis.** Single-channel current amplitude histograms were fitted with the sum of several Gaussian curves:

$$N = A \exp(-0.5((i - i_{\text{mean}})/s)^2) / (s(2\pi)^{0.5}), \quad (1)$$

where  $N$  is the number of events (samples),  $A$  is the area of the curve,  $i$  is the single-channel current,  $i_{\text{mean}}$  is the mean current, and  $s$  is the standard deviation. The single channel conductance,  $\gamma$ , was calculated as

$$\gamma = i/(V - V_{\text{rev}}), \quad (2)$$

where  $V$  is the absolute membrane voltage, and  $V_{rev}$  is the reversal potential. The open probability data,  $p_O$ , was fitted to a Boltzmann curve

$$pO(V) = 1 / (1 + \exp(-(V - V_{1/2})/s)), \quad (3)$$

where  $V_{1/2}$  is the midpoint potential, and  $s$  is the slope constant.

**Statistics.** Data are presented as mean  $\pm$  SEM. Statistical analyses were carried out with the one-way analysis of variance (ANOVA)-Fisher's protected least significant difference (PLSD) test, and the two-tailed Student's  $t$ -test.

## Concluding Remarks

We have found that pl-VDAC is activated in differentiated hippocampal neurons during apoptotic cell death and that block of this channel prevents apoptosis. Anion efflux through pl-VDAC appears to be critical for the progression of apoptosis in these cells, but not in NSCs that lack pl-VDAC channel activity. Instead, in NSCs an amiloride-sensitive  $\text{Na}^+$  channel is activated, playing a key role in the apoptotic process. These findings further improve our understanding of the diverse cell death mechanisms operative in the developing and the adult nervous system.

## Acknowledgements

We thank Peter Århem for sharing lab equipment, Sten Orrenius for interesting discussions and The MTP Network for a stipend to N. Akanda. This study was supported by grants from the European Commission (DEVNERTO, CT-2003-506143), the Swedish Research Council, Karolinska Institutet, Linköping University, and the County Council of Östergötland.

## References

- Yuan J, Shaham S, Ledoux S, Ellis HM, Horvitz HR. The *C. elegans* cell death gene *ced-3* encodes a protein similar to mammalian interleukin-1 beta-converting enzyme. *Cell* 1993; 75:641-52.
- Barbiero G, Duranti F, Bonelli G, Amenta JS, Baccino FM. Intracellular ionic variations in the apoptotic death of L cells by inhibitors of cell cycle progression. *Exp Cell Res* 1995; 217:410-8.
- Benson RS, Heer S, Dive C, Watson AJ. Characterization of cell volume loss in CEM-C7A cells during dexamethasone-induced apoptosis. *Am J Physiol* 1996; 270:1190-203.
- Bortner CD, Hughes FM Jr, Cidlowski JA. A primary role for  $\text{K}^+$  and  $\text{Na}^+$  efflux in the activation of apoptosis. *The Journal of biological chemistry* 1997; 272:32436-42.
- Yu SP, Yeh CH, Sensi SL, Gwag BJ, Canzoniero LM, Farhangrazi ZS, Ying HS, Tian M, Dugan LL, Choi DW. Mediation of neuronal apoptosis by enhancement of outward potassium current. *Science* 1997; 278:114-7.
- Colom LV, Diaz ME, Beers DR, Neely A, Xie WJ, Appel SH. Role of potassium channels in amyloid-induced cell death. *J Neurochem* 1998; 70:1925-34.
- Wang L, Xu D, Dai W, Lu L. An ultraviolet-activated  $\text{K}^+$  channel mediates apoptosis of myeloblastic leukemia cells. *The Journal of biological chemistry* 1999; 274:3678-85.
- Maeno E, Ishizaki Y, Kanaseki T, Hazama A, Okada Y. Normotonic cell shrinkage because of disordered volume regulation is an early prerequisite to apoptosis. *Proc Natl Acad Sci USA* 2000; 97:9487-92.
- Cain K, Langlais C, Sun XM, Brown DG, Cohen GM. Physiological concentrations of  $\text{K}^+$  inhibit cytochrome  $c$ -dependent formation of the apoptosome. *The Journal of biological chemistry* 2001; 276:41985-90.
- Hughes FM Jr, Bortner CD, Purdy GD, Cidlowski JA. Intracellular  $\text{K}^+$  suppresses the activation of apoptosis in lymphocytes. *The Journal of biological chemistry* 1997; 272:30567-76.
- Elinder F, Akanda N, Tofighi R, Shimizu S, Tsujimoto Y, Orrenius S, Ceccatelli S. Opening of plasma membrane voltage-dependent anion channels (VDAC) precedes caspase activation in neuronal apoptosis induced by toxic stimuli. *Cell Death Differ* 2005; 12:1134-40.
- Baker MA, Lane DJ, Ly JD, De Pinto V, Lawen A. VDAC1 is a transplasma membrane NADH-ferricyanide reductase. *The Journal of biological chemistry* 2004; 279:4811-9.
- Akanda N, Elinder F. Biophysical properties of the apoptosis-inducing plasma membrane voltage-dependent anion channel. *Biophysical journal* 2006; 90:4405-17.
- Colombini M, Blachly-Dyson E, Forte M. VDAC, a channel in the outer mitochondrial membrane. *Ion Channels* 1996; 4:169-202.
- Thinness FP, Gotz H, Kayser H, Benz R, Schmidt WE, Kratzin HD, Hilschmann N. [Identification of human porins I. Purification of a porin from human B-lymphocytes (Porin 31HL) and the topochemical proof of its expression on the plasmalemma of the progenitor cell]. *Biol Chem Hoppe Seyler* 1989; 370:1253-64.
- Jalonen T. Single-channel characteristics of the large-conductance anion channel in rat cortical astrocytes in primary culture. *Glia* 1993; 9:227-37.
- Bathori G, Szabo I, Schmehl I, Tombola F, Messina A, De Pinto V, Zoratti M. Novel aspects of the electrophysiology of mitochondrial porin. *Biochem Biophys Res Commun* 1998; 243:258-63.
- Guibert B, Dermietzel R, Siemen D. Large conductance channel in plasma membranes of astrocytic cells is functionally related to mitochondrial VDAC-channels. *Int J Biochem Cell Biol* 1998; 30:379-91.
- Bathori G, Parolini I, Szabo I, Tombola F, Messina A, Oliva M, Sargiacomo M, De Pinto V, Zoratti M. Extramitochondrial porin: facts and hypotheses. *Journal of bioenergetics and biomembranes* 2000; 32:79-89.
- Garty H, Palmer LG. Epithelial sodium channels: function, structure and regulation. *Physiological reviews* 1997; 77:359-96.
- Kellenberger S, Schild L. Epithelial sodium channel/degenerin family of ion channels: a variety of functions for a shared structure. *Physiological reviews* 2002; 82:735-67.
- Catterall WA, Goldin AL, Waxman SG. International Union of Pharmacology XLVII. Nomenclature and structure-function relationships of voltage-gated sodium channels. *Pharmacological reviews* 2005; 57:397-409.
- Colombini M. A candidate for the permeability pathway of the outer mitochondrial membrane. *Nature* 1979; 279:643-5.
- Shimizu S, Matsuoka Y, Shinohara Y, Yoneda Y, Tsujimoto Y. Essential role of voltage-dependent anion channel in various forms of apoptosis in mammalian cells. *J Cell Biol* 2001; 152:237-50.
- Bahamonde MI, Fernandez-Fernandez JM, Guix FX, Vazquez E, Valverde MA. Plasma membrane voltage-dependent anion channel mediates antiestrogen-activated maxi  $\text{Cl}^-$  currents in C1300 neuroblastoma cells. *The Journal of biological chemistry* 2003; 278:33284-9.
- Mannella CA. Minireview: on the structure and gating mechanism of the mitochondrial channel, VDAC. *Journal of bioenergetics and biomembranes* 1997; 29:525-31.
- Sabirov RZ, Okada Y. Wide nanoscopic pore of maxi-anion channel suits its function as an ATP-conductive pathway. *Biophysical journal* 2004; 87:1672-85.
- Rostovtseva T, Colombini M. VDAC channels mediate and gate the flow of ATP: implications for the regulation of mitochondrial function. *Biophysical journal* 1997; 72:1954-62.
- Sabirov RZ, Okada Y. ATP-conducting maxi-anion channel: a new player in stress-sensory transduction. *The Japanese journal of physiology* 2004; 54:7-14.
- Sabirov RZ, Sheiko T, Liu H, Deng D, Okada Y, Craigen WJ. Genetic demonstration that the plasma membrane maxianion channel and voltage-dependent anion channels are unrelated proteins. *The Journal of biological chemistry* 2006; 281:1897-904.
- Marin R, Ramirez CM, Gonzalez M, Gonzalez-Munoz E, Zorzano A, Camps M, Alonso R, Diaz M. Voltage-dependent anion channel (VDAC) participates in amyloid beta-induced toxicity and interacts with plasma membrane estrogen receptor alpha in septal and hippocampal neurons. *Molecular membrane biology* 2007; 24:148-60.
- Canessa CM, Horisberger JD, Rossier BC. Epithelial sodium channel related to proteins involved in neurodegeneration. *Nature* 1993; 361:467-70.
- Waldmann R, Lazdunski M.  $\text{H}^+$ -gated cation channels: neuronal acid sensors in the Na $^+$ /DEG family of ion channels. *Current opinion in neurobiology* 1998; 8:418-24.
- Chalfie M, Wolinsky E. The identification and suppression of inherited neurodegeneration in *Caenorhabditis elegans*. *Nature* 1990; 345:410-6.
- Driscoll M, Chalfie M. The *mec-4* gene is a member of a family of *Caenorhabditis elegans* genes that can mutate to induce neuronal degeneration. *Nature* 1991; 349:588-93.
- Waldmann R, Champigny G, Voilley N, Lauritzen I, Lazdunski M. The mammalian degenerin MDEG, an amiloride-sensitive cation channel activated by mutations causing neurodegeneration in *Caenorhabditis elegans*. *The Journal of biological chemistry* 1996; 271:10433-6.
- Bottenstein JE, Sato GH. Growth of a rat neuroblastoma cell line in serum-free supplemented medium. *Proc Natl Acad Sci USA* 1979; 76:514-7.
- Nicholson DW, Ali A, Thornberry NA, Vaillancourt JP, Ding CK, Gallant M, Gareau Y, Griffin PR, Labelle M, Lazebnik YA, et al. Identification and inhibition of the ICE/CED-3 protease necessary for mammalian apoptosis. *Nature* 1995; 376:37-43.
- Gorman AM, Hirt UA, Orrenius S, Ceccatelli S. Dexamethasone pre-treatment interferes with apoptotic death in glioma cells. *Neuroscience* 2000; 96:417-25.
- Norfleet AM, Thomas ML, Gametchu B, Watson CS. Estrogen receptor-alpha detected on the plasma membrane of aldehyde-fixed GH3/B6/F10 rat pituitary tumor cells by enzyme-linked immunocytochemistry. *Endocrinology* 1999; 140:3805-14.